Summer 2015

Histological and Immunohistochemical Analyses Used to Study Craniosynostosis in Pediatric Patients

Palvir Kaur Baadh
University of Akron Main Campus, pkb9@zips.uakron.edu

Histological and Immunohistochemical Analyses Used to Study Craniosynostosis in Pediatric Patients

Palvir Baadh, Phillip McClellan, BS, Robin Jacquet, MS, Ananth Murthy, MD and William Landis, PhD

The University of Akron, Akron, OH

Abstract

Craniosynostosis is a condition in which one or more of the sutures of the skull grow together (fuse) earlier than normal in infants. Sutures are large gaps located at the bony plates or joints of the head. Craniosynostosis causes the skull to expand and grow in the direction of any normal open suture, creating craniofacial complications, such as drooping eyelids and abnormal intracranial pressure, head shape, or brain morphology. This premature fusion or ossification of sutures affects approximately 300-500 live births in 1,000,000 (Kolpakova-Hart *et al.*, 2008) with considerable variation in phenotype, depending on which suture(s) is involved. Corrective surgery can be performed to reshape the skull and eliminate the symptom(s) present in the infant. There is no known cause of craniosynostosis or direct pattern of heritability from parent to affected infant and the condition can appear syndromically (associated with syndrome or condition) or non-syndromically. However, the majority of cases reported are sporadic, non-syndromic cases, in which pediatric patients suffer

from premature fusion of only one suture (Levi *et al*., 2012). In the current prospective study, histological and/or immunohistochemical analyses have been conducted on sagittal synostoses as well as patent (normal open suture) tissue from the skulls of three pediatric patients. Patient surgeries were performed at Akron Children's Hospital. The studies were begun to understand more completely the underlying etiology and possible risk factors of non-syndromic craniosynostosis. Histological staining, including toluidine blue, hematoxylin and eosin, and picrosirius red counterstained with alcian blue, has been performed for qualitatively describing tissue and cell architectural shapes and gross morphology. Immunohistochemical analysis has also been performed to study the presence of osterix, a transcription factor essential for osteoblast differentiation and bone formation. Analytical results of this work are ongoing.

Introduction

Craniosynostosis may affect any of the bones of the human skull. Eight bones form the neurocranium, which is sometimes referred to as the braincase. These bones include the single frontal, occipital, sphenoid, and ethmoid bones and two parietal and temporal bones. These bones together form the protective case around the brain. The ossification of these flat bones of the skull occurs when mesenchymal cells differentiate into bone cells (osteoblasts) through intramembranous ossification, that is, ossification that occurs from fibrous membranes (Levi *et al*., 2012). These bones are integrated and unified;

yet conversely separated by fibrous sutures, where the different bone plates meet.

The skull of an infant has four sutures, which include the metopic, coronal, sagittal, and the lambdoid suture. The metopic suture is located where the two frontal bones on both sides of the skull meet. This suture extends from the top of the head to the middle of the forehead. The coronal suture occurs where each frontal bone meets the parietal bones on both sides of the head. This suture extends from left-most side of the skull to the right-most side of the skull (ear to ear). The sagittal suture occurs where the two parietal bones meet. It extends from the middle of the head to the back. The lambdoid suture is found where each parietal bone meets the occipital bone. This suture extends across the back of the head horizontally. The suture joints are synarthroses (joints having little or no movement). During childbirth, they are flexible enough to allow the skull bones to overlap and absorb mechanical stresses as the baby passes the birth canal, avoiding damage to the brain (Bronfin, 2001). All four sutures are very important to the growth of the skull and the brain in the early stages of life. The patency of these sutures allows brain expansion and formation of the neurocranium (Levi *et a*l., 2012). If fusion occurs prematurely — before birth or at birth — between the sutures, the growth of the neurocranium and brain will not proceed correctly because the centers of growth in the skull are ossified (in other words, they have become closed). Such a condition is termed craniosynostosis. It is the premature fusion of one or more of the sutures, which are spaces or gaps between the bones that comprise the human skull. Surgical intervention of

the deformity is the only form of treatment to correct premature suture fusion. If the deformity is not corrected, it will worsen, threatening both the aesthetics and functional components of the skull of the child.

Nonsyndromic synostoses, those occurring without syndrome, are the most prevalent form of the craniosynostosis abnormality, affecting the coronal, sagittal, metopic, or the lambdoid suture or occurring through a combination of the sutures. Normal development of the skull (calvarium) is dependent on skeletal bones and synchronized expansion of the brain. Interactions between the bone plates of the skull, brain, suture mesenchyme, and outer covering of the head, the dura mater, allow for proper skull growth. It is not known which interactions are affected in the calvarium that lead to the craniosynostosis phenotypes in infants. Many mouse and rabbit studies have been conducted to understand this condition to a better degree, but suture biology is yet largely uncertain. The exact causative pathways that lead to the condition remain to be discovered and thoroughly understood.

Research studies focusing on potential causes of nonsyndromic premature suture closure suggest a variety of factors that could be contributing to the diseased state, including hereditary, environmental, and/or biomechanical factors. Extensive research has been done in studying the mutations in proteins or transcription factors found in craniosynostosis-diseased infants. Causative mutations in the fibroblast growth factor (FGF), transforming growth factor beta (TGFß), and twist (TWIST1) families as well as runt-related transcription factor 2 (RUNX2), osteoblast-specific signaling proteins and transcriptions factors (TFs)

have each been identified individually in studies using nonhuman models and have been linked to craniosynostosis pathology (Connerney *et al*., 2008 and Morriss-Kay *et al*., 2005). Of particular interest to the study researched here is a novel zinc-containing transcription factor, osterix, which is essential for osteoblast differentiation and bone formation and has not been investigated previously in human tissue.

Osterix is a transcription factor (Sp7) fundamental for osteoblastogenesis and bone formation in mice (Zhu *et al*., 2012). Null mouse mutants that lack osterix will die just hours after birth because there is a deficiency in intramembranous and endochondral ossification in their bodies (Baek *et al*., 2009). The consequence of death is indicative of the significance of osterix and its role in vertebrate bone formation. Genomic studies also show that osterix is responsible for bone density in humans (Zhu *et al*., 2012).

Osterix-expressing cells produce Wnt protein and respond to Wnt signaling (Tan *et al*., 2014). Wnt represents both a signaling molecule and a signaling pathway and Wnt critically regulates bone development. It has been shown that, if Wnt secretion in vivo is inhibited, inappropriate bone differentiation and diminished bone proliferation take place along with a reduction in Wnt signaling. Consequently, osterix-expressing cells produce Wnt proteins that induce Wnt signaling responses regulating proliferation and differentiation of bone (Tan *et al*., 2014). Furthermore, recent craniosynostosis research conducted at the University of Pittsburgh studied development of the skull bones of mice in response to increased Wnt signaling (Szabo-Rogers *et al*., 2014).

The work found that differentiation of osteoblasts and osteogenesis were increased in the mouse frontal bones (Szabo-Rogers *et al*., 2014). These findings are very important to this present craniosynostosis study because they suggest that, if osterix inactivation can lead to delayed osteoblast maturation and reduced bone formation in mice, perhaps the overexpression or up-regulation of the osterix transcription factor can affect Wnt signaling. This possibility could lead to increased osteoblast differentiation and formation of bone. In this manner, osterix can play a significant role in early vertebrate suture formation.

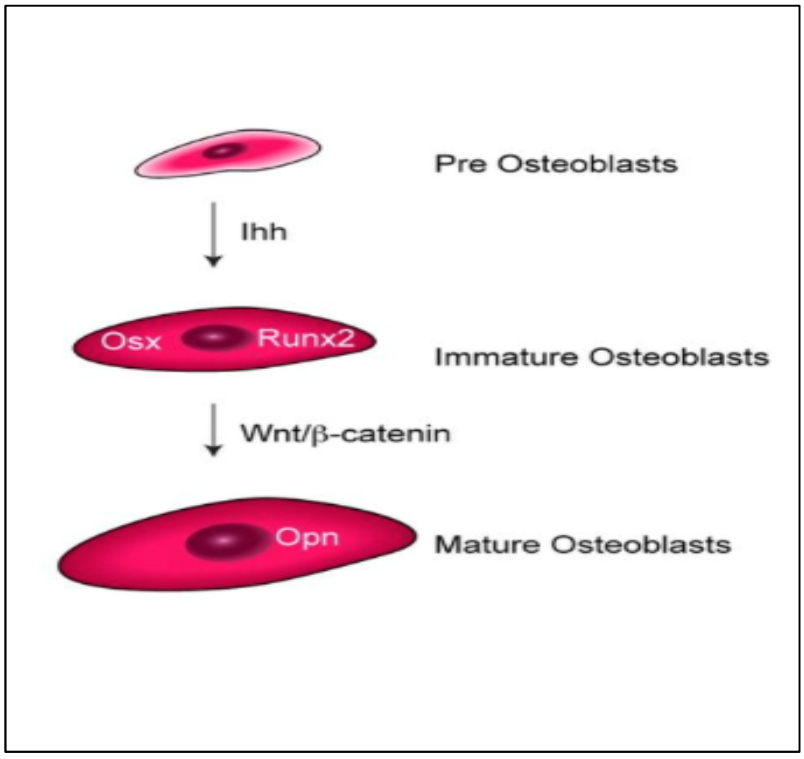

Figure 1: A schematic diagram showing that Wnt signaling occurs after the expression of osterix for mature osteoblast differentiation (Day and Yang, 2008).

The goal of this project is to investigate the morphology, structure, and biochemistry of fused suture sites by using light microscopy, histology and immunohistochemistry (IHC). The specimens to be investigated are affected sagittal synostosis tissues and unaffected, open coronal tissues (controls) from infants of different ages. For histology, various stains were utilized to facilitate microscopic study and identification of cellular components and arrangement of cells inside the diseased craniosynostosis and normal samples. The stains were also applied in some cases to provide biochemical information about the samples.

Toluidine blue was the principal stain used. It highlights nuclei acids such as DNA and RNA because it is a basic thiazine metachromatic dye with high affinity for acidic tissue components. As such, toluidine blue can distinguish between tissues, in this case, the scaphocephaly (sagittal synostosis) and open sutures (control). Hematoxylin and eosin was another stain used in this analysis. Hematoxylin stains nuclei of cells a deep blue color and binds to basophilic substances. The counterstain, eosin, binds to acidophilic substances such as proteins and cytoplasmic material and turns them red or pink. Compared to a single stain, counterstains provide better visualization of cells and cell structures. A picrosirius red and alcian blue stain was also applied. Picrosirius red allows histological visualization of both Type I and II collagen, whereas alcian blue stains acidic polysaccharides, for example, glycosaminoglycans in cartilaginous bones.

IHC examination of osterix transcription factor was conducted in the diseased tissues. IHC is a method of applying antibodies for identifying proteins specific to a histological sample, in this case the affected and normal sutures. By using IHC methods, the identification and the presence or location of the osterix transcription factor in tissue sections were made through antibody binding to this protein. These histological and IHC studies have demonstrated thorough investigation of the tissues in question and provided scientific insight into the pathology.

Material and Methods

Cranial suture specimens were obtained from craniosynostosis patients who underwent corrective surgery at Akron Children's Hospital, Akron, OH. Affected and normal tissue from the skull were collected and used for research purposes in compliance with Hospital regulation and approval from the parent(s) of the patients. Sagittal suture specimens from three different patients were collected over the course of two years (2013-2014). The ages of the patients were two (Specimen 3) and four months (Specimen 4) with one age unknown (Specimens 1 and 2). All patients suffered from nonsyndromic craniosynostosis and were sporadic (unpredicted) cases. Specimens 1-2 were taken in surgery at the Akron Children's Hospital in May, 2013, and placed in 10% neutral buffered formalin (NBF, VWR, Radnor, PA) at 4℃ until research studies were begun two months later in the Department of Polymer Science at the University of Akron. Specimen 3 was obtained in July, 2013, and also stored in NBF at 4℃ until histological

analyses were performed in November of the same year. Specimen 3 was obtained from a male, three-month-old child. Specimen 4 from a four-month-old male was received in April, 2014, and stored in NBF at 4℃ until histological analyses were conducted weeks later.

Histological Analyses

Sample dimensions and location. Specimens 1-4 were each of different sizes and shapes obtained from surgery. They were measured in length and width as 4 cm X 0.5 cm, 2 cm X 0.5 cm, 12 cm X 5 cm, and 9.5 cm X 3.5 cm, respectively. Specimens 1-4 were all sagittal synostoses; specimen 3 also contained open coronal and lambdoid sutures; and specimen 4 contained an open coronal suture. The open coronal and lambdoid sutures in specimens 3-4 were unaffected by the synostosis and served as experimental controls to the affected, closed (fused) sagittal regions.

Based on the tissue appearance and its hardness, specimen 1 was subdivided with a scalpel blade into three regions: ossified, partially ossified, and lacking ossification. Specimen 2 was similarly divided, but only into ossified and partially ossified regions because of its short length. Specimen 3 was divided into five areas of interest, sagittal anterior and posterior (partially ossified), sagittal center (ossified), and a coronal and lambdoid region. Specimen 4 was cut into ten areas, six sagittal and four coronal. Of the sagittal sutures, three adjacent regions (anterior, central, and posterior) were themselves subdivided equally into anterior and posterior portions. Of the coronal sutures, two opposing regions

were each subdivided equally into medial and lateral portions. Images of some of the specimens are shown below.

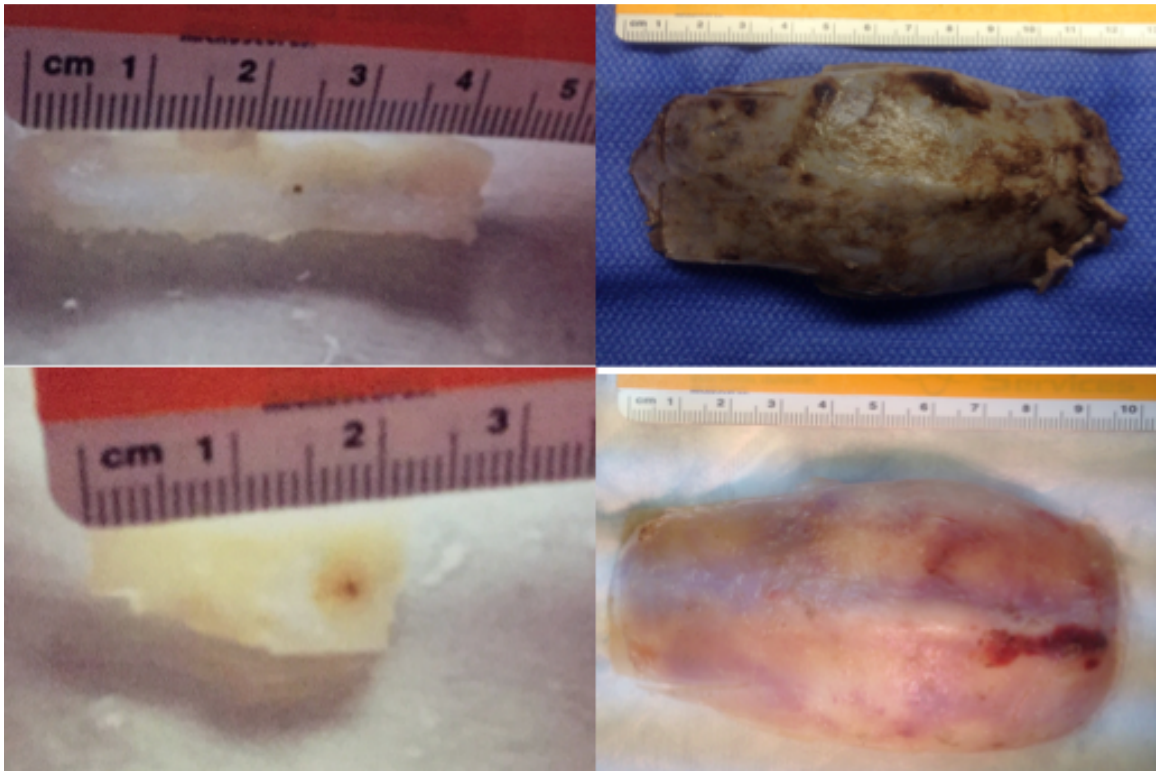

Figure 2: Photographs illustrating general overview of specimen 1 (upper left panel), specimen 2 (lower left panel), specimen 3 (upper right panel), and specimen 4 (lower right panel) obtained following surgery. Samples were later subdivided and processed.

Fixation and decalcification. Specimens 1-4 were each fixed in 10% NBF at 4℃. Specimens 1 and 2 were fixed for approximately two months and specimens 3 and 4 were fixed for 4 months and 1 month, respectively. Specimens were then divided using a scalpel blade (Specimen 1 and 2) or a Dremel Rotary Tool (Bosch Corp., Stuttgart, Germany) (Specimen 3 and 4) into their individual parts based on sample hardness and appearance. Following fixation, all specimens were divided as described above. NBF solution was

removed from all divided specimen samples with deionized water (DI H_2O). Three washes, ten minutes each, were used with a rotary shaker (Rotoshaker Genie, Scientific Industries, Bohemia, NY). After the final wash was finished, 70% ethanol (Cat. No. 2701, Decon Laboratories, Inc., King of Prussia, PA) was added to the containers holding the several divided specimen samples. Containers were stored in a 4℃ refrigerator until the following day when the washes were repeated. Samples were decalcified initially in 100% Immunocal (Decal Chemical Corp., Sufferin, NY) for 24 (samples from Specimens 1 and 2) or 72 hours (samples from Specimens 3 and 4) on the rotary shaker at room temperature. Hardness of each tissue sample was detected with a needle and samples were decalcified further if they were hard. To complete the decalcification process, a 50:50 solution of Immunocal and NBF was prepared, and samples were transferred from 100% Immunocal to the 50:50 solution. Samples from Specimens 1-2 and 3-4 were additionally decalcified 1.5 and 24 hours, respectively. Samples were tested again with a needle to detect hardness of the suture tissue and were found to have decalcified adequately. To remove Immunocal-NBF solution, three DI H_2O washes, fifteen minutes each, were done using the rotary shaker and three, 70% ethanol washes, fifteen minutes each, removed the remaining water. The samples were stored in the last ethanol wash at 4℃.

Processing. The processing steps were identical for all samples. Samples were removed from the 4℃ refrigerator and from their containers having 70% ethanol. Samples were placed into plastic cassettes, which were labeled to

identify their individual tissue and its corresponding region. The cassettes were next placed into a tissue-processor (Leica Asp 300s, Buffalo Grove, IL) and left over the weekend to complete the processing cycle of a series of automated washes in preparation for sample embedding.

Embedding. The embedding procedure was the same for all samples. After processing, individual tissues were quickly removed from the processor and immediately embedded into paraffin wax blocks using a tissue embedder (Leica EG 1150C, Buffalo Grove, IL). Samples were embedded in wax molds with their anterior portion (in relation to the anatomy of the skull) at the bottom of the mold. This orientation was necessary so that, when serial sections were prepared, they would be cut anterior-to-posterior and their regional identity would be recognized. The thinnest dimension of each sample was also oriented toward the bottom of the mold. After wax was poured over the samples, embedded molds were set on a cooling plate (Leica EG 1150C, Buffalo Grove, IL) to allow the wax to solidify. After ten minutes, hardened paraffin wax blocks containing the samples were stored in a -20℃ freezer to allow the blocks to harden.

Sectioning. Samples were all treated identically when sectioning. Wax blocks were removed from the -20℃ freezer and placed in a -80℃ freezer to supercool wax blocks overnight before sectioning. This procedural step helped harden the blocks and aided sectioning. Wax blocks were then removed from -80℃ and were sectioned using an automated microtome (Leica RM 2255, Buffalo Grove, IL). Sections were cut at 6 μm thicknesses using a tungsten carbide blade. Wax blocks were trimmed and then serial (consecutive) sections

were prepared. Surface decalcification was utilized for blocks that produced shredded sections. Sections were floated on a water bath (Leica HI1210, Thermo Scientific, Portsmouth, NH) and then transferred to Superfrost Excell slides (Thermo Scientific, Portsmouth, NH). Slides were labeled accurately and allowed to dry in air overnight in a vertical position.

Staining. Various basic stains were used to highlight and examine structural components of the suture tissue. The stains utilized in this study were hematoxylin and eosin, toluidine blue, pircosirus red, and pircosirus red counterstained with alcian blue.

Preparation of Stains. Hematoxylin and eosin (H&E) stain was applied to samples obtained from specimens 1 and 2 (Figure 2). Hematoxylin is a stain used for nuclear detail, while eosin serves as a contrasting counterstain for extracellular substances. A progressive staining procedure was used in which slides were stained with hematoxylin, rinsed, and then counterstained with eosin. The following materials were used to prepare the H&E stain: Hematoxylin, eosin Y, weak acid deionized H_2O (0.3% HCl), and weak basic NH_4OH (0.5% NH_4OH; also known as bluing agent). These reagents were mixed over a stir plate and then stored at room temperature.

Toluidine blue (T-blue) stain was used for samples obtained from specimens 1 and 2 in this study. Toluidine blue is a thiazine metachromatic dye that stains acidic tissue components. This dye stains nucleic acid material blue and polysaccharides purple. For this stain 0.1% toludine blue solution was made. Toluidine blue powder (FisherBiotech, Fair Lawn, N.J.) was measured to 0.5 gm

and 500 mL of milliQ water was added. Stain was then mixed over a stir plate and stored at room temperature.

Picrosirus red (PSR) was another stain utilized in this study. Staining was performed on samples obtained from specimen 1 and 2. PSR is intended for visualization of collagen fibers (types I and II). Collagen stained with PSR is visible by both normal and polarized light microscopy (birefringence). PSR stains collagen fibers red and cell cytoplasm and muscle fibers yellow. For preparation of this stain, Sirius red F3B (C.I. 35780, Pfaltz and Bauer Inc., Waterbury, CT) was measured to 0.5 gm and 500 mL of an aqueous solution of picric acid was added and mixed on a stir plate. Acidified water was also prepared by measuring 5 ml of acetic acid and adding it to 995 mL of deionized water.

Picrosirus red and alcian blue stains were utilized for samples obtained from specimen 3 (Figure 2). The purpose and preparation of picrosirus red stain are explained in the previous paragraph. Alcian blue stain is intended for visualization of sulfated and carboxylated acid mucopolysaccharides and sulfated and carboxylated sialomucins (glycoproteins). A 3% glacial acetic acid solution was prepared by adding 9 mL of acetic acid to 300 mL of deionized water. The 3% acetic acid solution was added to 3 gm of Alcian Blue 8GX powder (Sigma Chemical Co., St. Louis, MO), creating a 1% alcian blue solution. The solution was then mixed over a stir plate and pH adjusted to 2.5 using acetic acid. Stain was then stored at room temperature.

Staining procedure.

Deparaffinizing, clearing and hydration. All prepared slides were placed in an oven at 58℃ for a minimum of 2 hr to deparaffinize sections. Three changes of xylene (EK Industries, Joliet, IL) washes, 5 min each, were carried out in the fume hood. A change of 100% ethanol for 2 min was then done, followed by a 95% ethanol wash for 2 min. Two changes in 70% ethanol were done for 2 min each. Distilled water rinse for 2 min followed.

Staining process for hematoxylin and eosin. Slides were stained in filtered hematoxylin for 5 min and then destained in 0.5% HCI (freshly prepared in water) for 20 sec. Slides were then briefly rinsed in running deionized water and slides were dipped in water five times. Slides were then washed in 0.5% ammonium hydroxide (bluing agent) for 30 sec, which was also freshly prepared. Slides were then washed in 95% ethanol for two min. The counterstain eosin Y was then applied for 1 min.

Staining process for toluidine blue. Slides were immersed in freshly filtered 0.1% T-blue stain for 1 min. Slides were then dipped in freshly distilled water five times.

Staining process for picrosirius red. Slides were placed in a staining dish containing picrosirius red stain for 1 hr. Slides were then washed in two changes of acidified water for 2 min each.

Staining process for picrosirus red and alcian blue. Slides were placed in 0.5% acetic acid solution for 10 min, removed, and then placed in 1% alcian blue stain (pH 2.5) for 10 min. Two washes of 0.5% acetic acid solution followed for 3

min each. Slides were placed into a staining dish containing 0.5% picrosirius red counterstain for 1 hr. Two 0.5% acetic acid rinses (ten dips) were then performed.

Dehydration, clearing and mounting slides. After completing the staining process, two changes of 95% ethanol for 1 min each were conducted. Two changes of 100% ethanol for 1 min each followed. Slides were put through three xylene washes (5 min each) before being mounted and coverslipped with DPX Mounting Medium (Cat. No. 13512, Electron Microscopy Sciences, Hatfield, PA). Slides were allowed to dry overnight in a horizontal position before microscopic examination.

Immunohistochemistry for paraffin-embedded tissue sections (IHC). This technique was applied to samples obtained from specimen 4 (Figure 2). IHC detects an antigen (protein of interest in cells) in tissue sections by antibody binding. IHC provides the identification of the location and distribution of specific proteins in the tissue section. In this research analysis, the osterix protein was studied by IHC.

Deparaffinizing, drying, rehydration and fixation. Prepared slides were placed in an oven at 58℃ for 4 hr to deparaffinize the sections. Three changes of xylene (EK Industries, Joliet, IL) washes, 10 min each, were carried out in a fume hood. Two changes of 100% ethanol for 5 min each were done. Slides were then placed into 95% ethanol twice for five minutes each. Slides were then removed from solution and placed on a countertop and dried with a heat gun (cold air setting) for 10 min. The heat gun setting was changed to hot air and

slides were dried for additional 10 min. The cold-hot drying was repeated for 5 min each to complete this four-process sequence. Two changes of milliQ water followed for 5 min each to rehydrate the sections. Slides were then placed in 10% NBF for fixation overnight at room temperature.

Epitope (antigen) retrieval. Slides were removed from NBF solution and two changes of deionized water, five minutes each, were made. Two 100% Immunocal washes (1 hr each) followed. Again, slides were washed twice with deionized water for 5 min each. Slides were then placed into a dish containing epitope retrieval solution (see below) and the dish was placed in a 60℃ water-bath for 72 hr.

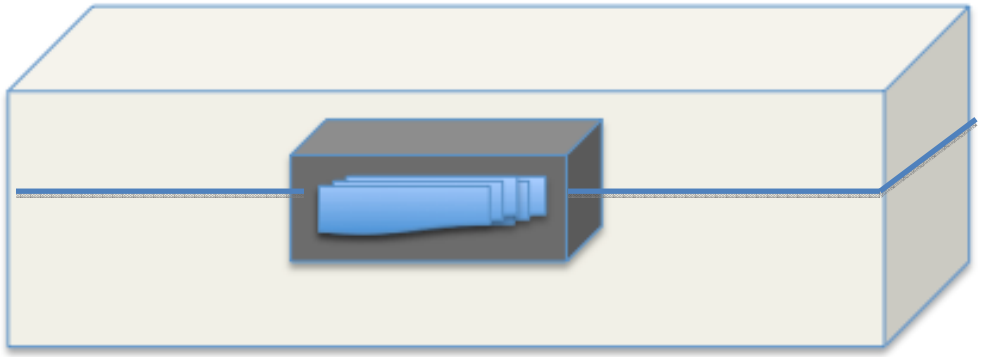

Figure 3: Illustration of slides (blue) in a covered staining dish (dark grey box) containing epitope retrieval solution. The slide box sits in a water bath, heated to 60℃, within a larger box (light grey). The blue line in the illustration indicates the water level.

The water in the bath was checked during the 72 hr time frame to maintain its appropriate level. Epitope retrieval solution was prepared by adding 1.47 gm of sodium citrate, 0.37 gm of ethylenediaminetetraacetic acid (EDTA), and 0.25 mL

of Tween 20 to 500 mL of H_2O and with stirring on a stirplate. The pH was adjusted to 6-6.5. hydrogen chloride.

Application of primary antibody. Slides were cooled by adjusting the water bath to 20℃. Slides were maintained in a hydration state for further processing. Slides were washed twice with phosphate-buffered saline (PBS) solution for 5 min each. Slides were removed from PBS and placed individually on a countertop. Two-three drops of Background Buster Blocking Agent (Innovex Biosciences, Richmond, CA) were immediately applied to the slides for 30 min to block endogenous tissue sites of possible antibody binding. The blocking agent was removed quickly by drainage from the slide and primary osterix antibody (dilution factor: 50 micrograms of antibody to 1 mL of diluent) was applied. Other slides were processed in the same manner except that they were treated with Tris-buffered saline and Tween 20 (TTBS) in place of the osterix antibody (these slides served as negative controls). Slides were left overnight at 4℃.

Peroxide/Methanol block, DAB, hematoxylin staining, and mounting slides. Three washes of TTBS were applied for 5 min each. ImmPress Reagent Peroxidase (2^{nd} antibody) (Vector, Burlingame, CA) was applied to all slides for 30 min. Again, three washes of TTBS identical to those noted above were performed. A 30% methanol hydroxide and 0.3% hydrogen peroxide (H_2O_2) block for applied for 10 min. Three TTBS washes followed for 5 min each. 3,3-diaminobenzidine (DAB) peroxidase was applied to slides for up to 2 min. Once brown coloration was seen on slides, DAB was removed and slides were quickly placed in a dish containing PBS solution. To prepare DAB peroxidase, a

MaxTag DAB tablet (Rockland Immunochemicals, Inc., Gilbertsville, PA) was added to a non-light-penetrating test tube and PBS was added to the 7 mL mark of the tube. DAB was dissolved thoroughly in PBS solution and stored on ice until needed for use. Immediately prior to application, 2-3 drops of H_2O_2 (activator of DAB) were added to the test tube and the tube was shaken. Slides were then washed with PBS two times for 5 min each. Mayers hematoxylin (Cat. #26252-01, Electron Microscopy Sciences, Hatfield, PA) was used to stain slides for 1 min. Slides were placed under running deionized water for 4 min. Slides were then dipped in bluing reagent ten times consecutively. The following alcohol washes were then used in order: two 70% ethanol washes, two 95% ethanol washes and two 100% washes. Each wash was timed for 2 min. Three xylene washes were then used, each 5 min. Slides were mounted and coverslipped and left to dry in a vertical position.

*Microscopy***.** In this study, an Olympus 1X70 (Olympus America, Center Valley, PA) light microscope combined with Olympus MicroSuite Software for Imaging Applications was utilized to view sections. Slides were cleaned with a KimWipe (Kimberly-Clark Professional, Roswell, GA) and then placed on the microscope stage. The large and small coarse focus knobs of the microscope were adjusted until the image appeared clear. Adjacent areas of each slide were scanned and imaged section-by-section and saved onto a USB drive. Images were taken at 4X magnification and a scale bar was superimposed on each image. Saved images were stitched together using Microsoft Image Composite Editor and montage images were compiled and stored. Sufficient overlap

between images was maintained for proper stitching of consecutive images. Stitching images in this manner helped maintain clarity of the full section and its resolution.

Results

Basic dyes such as T-blue, H&E, and PSR were used to assess craniosynostotic diseased tissue obtained from the specimens of interest, in this case specimens 1 and 2. Results indicated different patterns of morphology between specimen areas that were identified as ossified, partially ossified, and absent of ossification. These regions were classified based on their position and location in relation to the anatomy of the skull before being dissected and sectioned. The ossified regions of specimens 1 and 2 were osteogenic centers that had undergone premature fusion of the skull. These center-ossified regions were of particular interest in this study and therefore they were compared to the other two skull areas (partially ossified and absent of ossification) to study regional differences in bone anatomy. Figure 4 shows that bone in the ossified skull region had more marrow space in comparison with it counterparts and also demonstrated that osteocytes trapped in lacunae were more numerous and indicative of ossification in these samples. Below are images of the various stains of specimens 1 and 2 showing gross morphology and anatomy of the affected suture tissue.

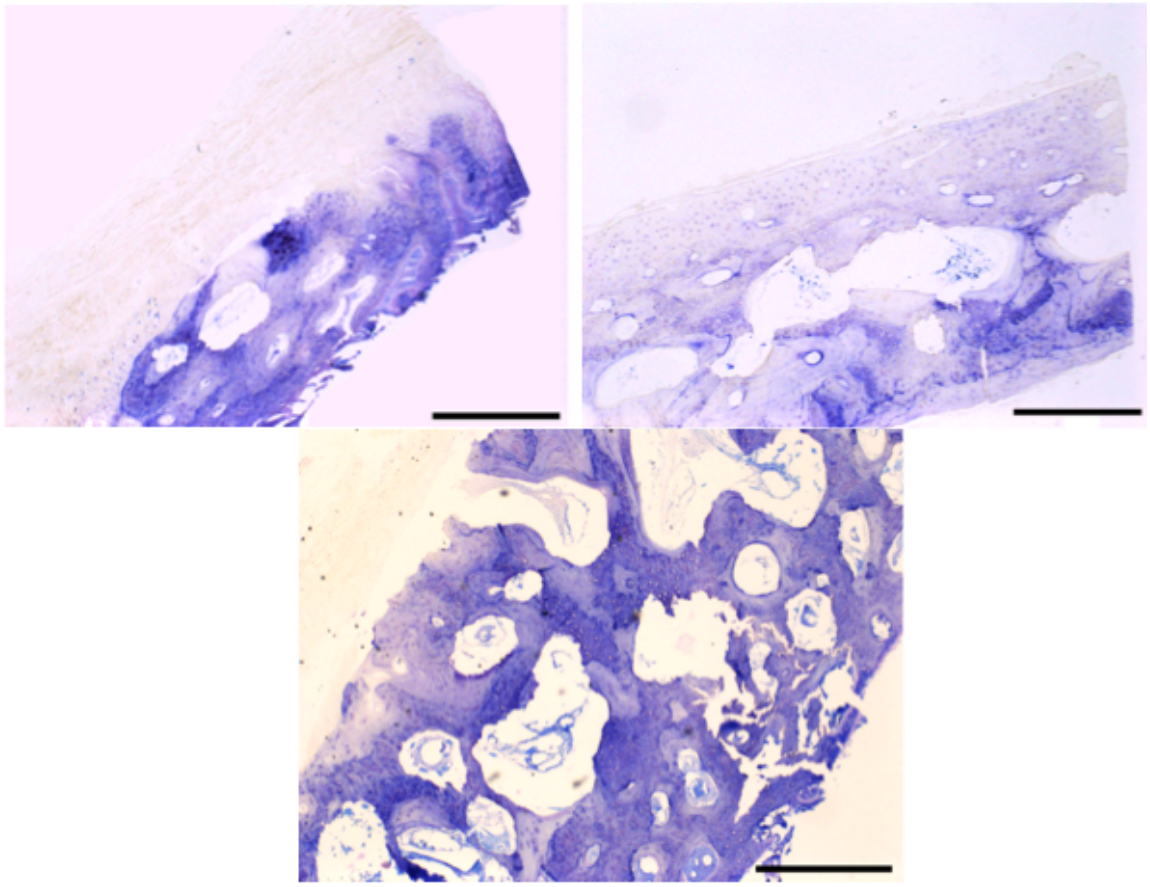

Figure 4: T-blue-stained images of specimen 1 depicting three different regions of the sagittal suture from a patient of unknown age or gender. Top left: There is little or no ossification in this part of the specimen. Top right: Another area of the same specimen is partially ossified as determined by its hardness. Bottom center: A third area of the specimen is ossified, again determined by its hardness. T = Trabeculae, M = Mineral. Scale bar in all images = 500 μm.

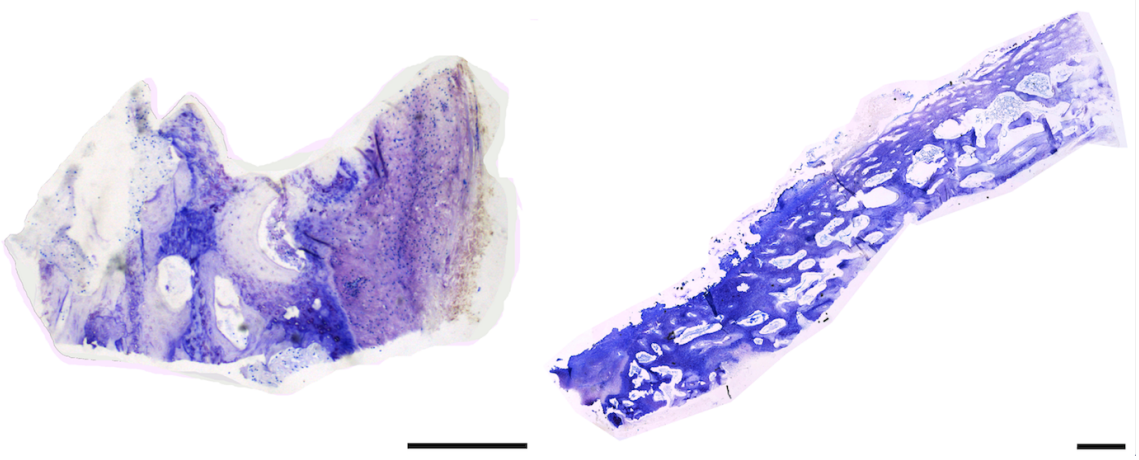

Figure 5: T-blue stained images of specimen 2 (obtained from a patient of unknown age and gender) depicting a partially ossified (left) and ossified region (right) of the suture. Both images show the fully transverse suture region. Right image is a series of separate photomicrographs that have been stitched together with ICE Software. Scale bars in left and right image are 500 μm and 1 mm, respectively.

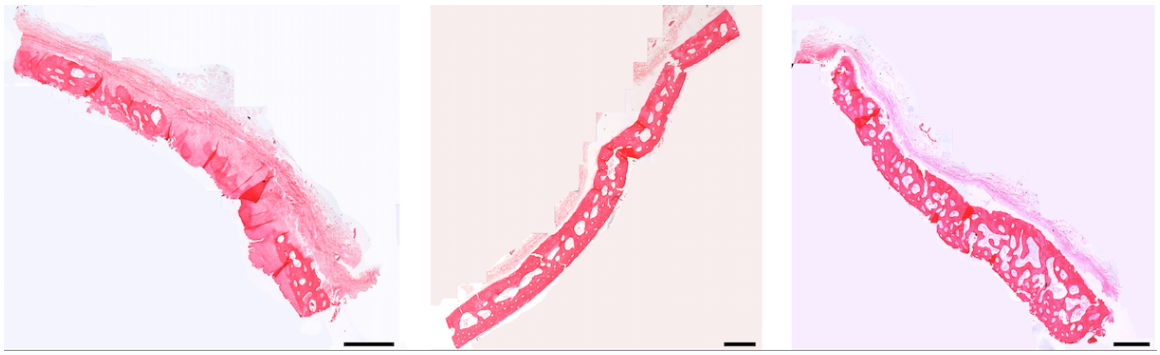

Figure 6: H&E-stained images of Specimen 1 taken from different areas of suture tissue. The left, middle, and right images, each stitched from numerous photomicrographs, display an area absent of ossification, a partially ossified region, and an ossified region, respectively. Scale bar in all images = 1 mm.

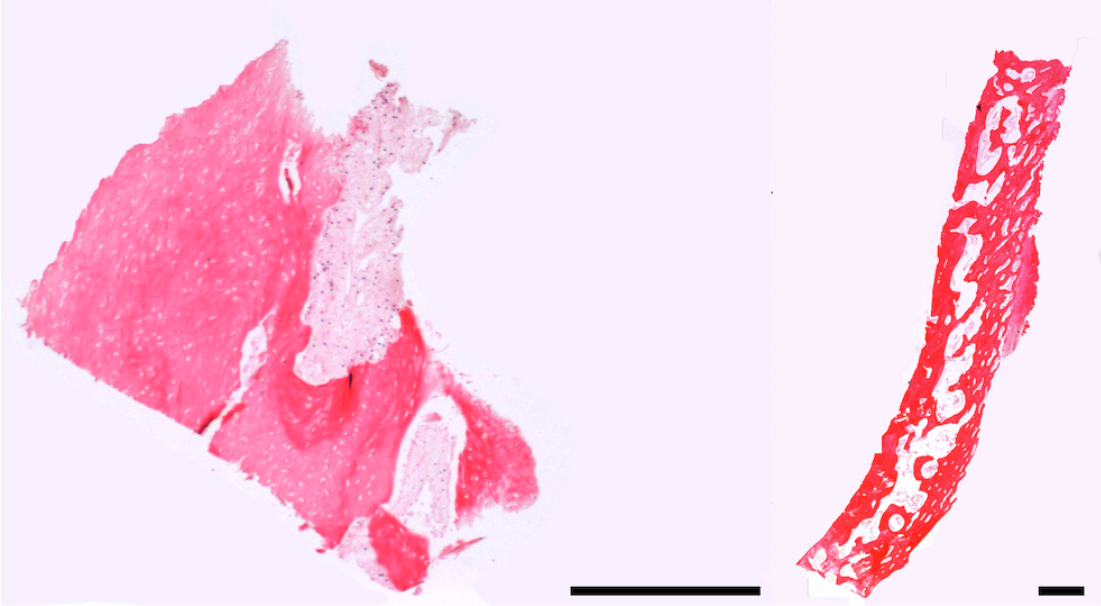

Figure 7: H&E-stained images of specimen 2 illustrating a partially ossified (left) and an ossified region (right) of the suture tissue. The left side of the ossified image faces the dura mater of the skull, while the right side faces the skull periosteum side. Scale bars in left and right image are 500 μm and 1 mm, respectively.

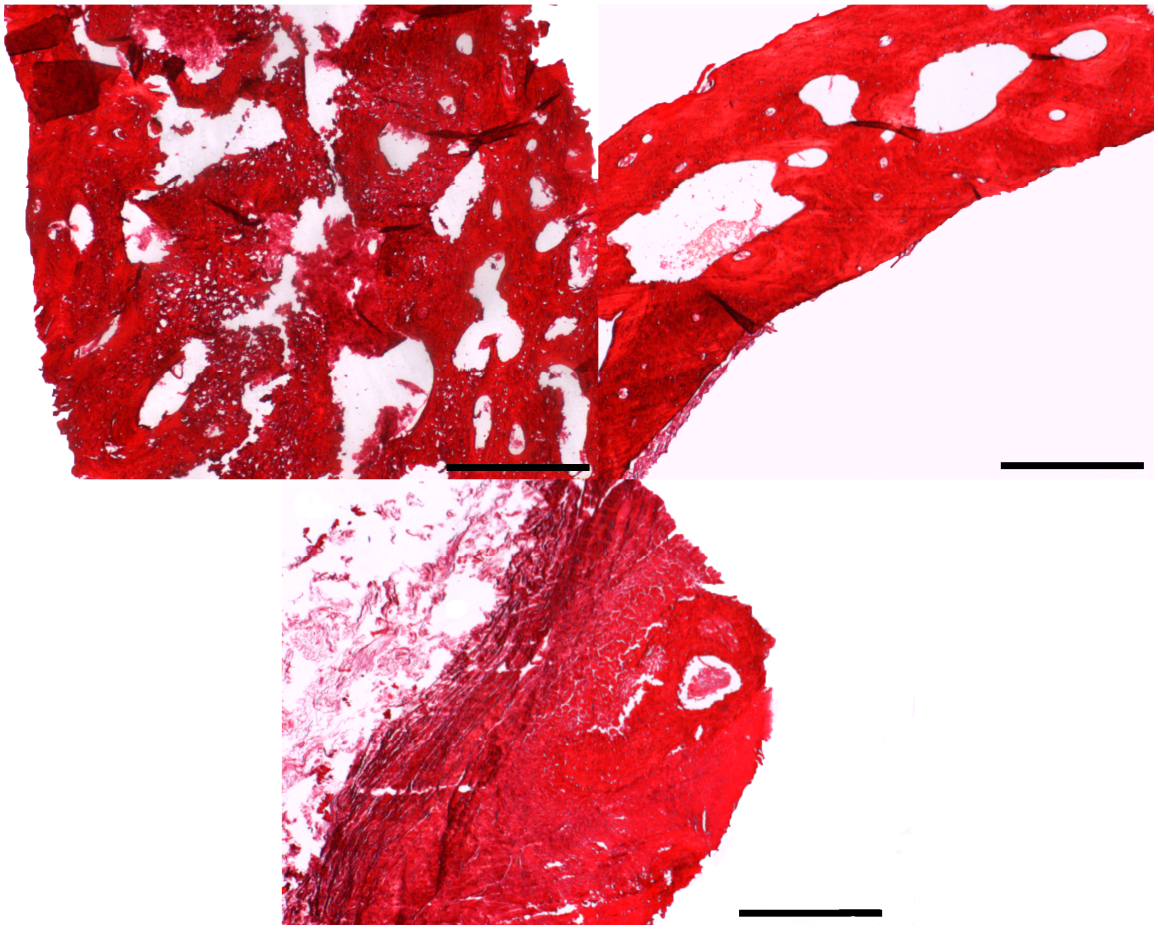

Figure 8: PSR-stained images of specimen 1 showing particular areas of suture tissue, an ossified region (top left), a partially ossified region (top right) and an area lacking ossification (bottom center). Scale bar in all images = 500 μm.

In all stained ossified, closed regions obtained from sagittal sutures, mineralized bone trabeculae were more apparent than in stained partially ossified regions and regions absent of ossification. Partially ossified regions and regions absent of ossification displayed fibrous tissue having little or no trabecular formation, an observation indicating that areas have not fully undergone intramembranous ossification. Trabecular bone, also known as cancellous bone,

is usually highly vascularized, a fact which explains the large marrow spaces in the ossified regions compared to the other two regions (Figure 8). Flat bones, such as those of the skull, receive a superficial blood supply from the periosteum, which is needed for proliferation of bone cells. This additional fact could be the very reason that many marrow spaces are present in the ossified regions indicative of blood vessels and capillary blood supply needed for growth.

In Figure 7, the ossified region displayed an interesting pattern at its periosteum side. The mineralized bone trabeculae appeared to follow a particular arrangement and run parallel to each other. The architecture and arrangement of the bone tissue seemed unique in the sense that small-elongated holes line the periosteum surface and gradually diminish in size deeper into the tissue. These holes near the periosteal surface of the suture were different from the deepest tissue regions where prominent large holes form trabecular bone. The reasons for the presence of these two distinct types of holes in the sutures are not clear, but the differences between the periosteum and trabecular bone could be where underlying premature ossification originated because of mechanical stress on the suture tissue.

Suture fusion results from intramembranous ossification. This process includes the appearance of an ossification center in the fibrous connective membrane region and secretion of bone within the fibrous membrane to form woven bone (immature trabecular bone). Woven bone is later remodeled to create lamellar bone (mature bone). Figure 9 shows both lamellar and trabecular bone. The lamellar bone in this figure appeared organized and stress-oriented,

two characteristics of lamellar bone in general. Moreover, when the ossified region of specimen 2 was viewed under higher magnification using a polarized light microscope, lamellar organization reflected a repeating pattern of bright and dark bands of collagen fiber architecture. This patterning is suggestive of mature lamellar bone present in the tissue sample (Figure 10).

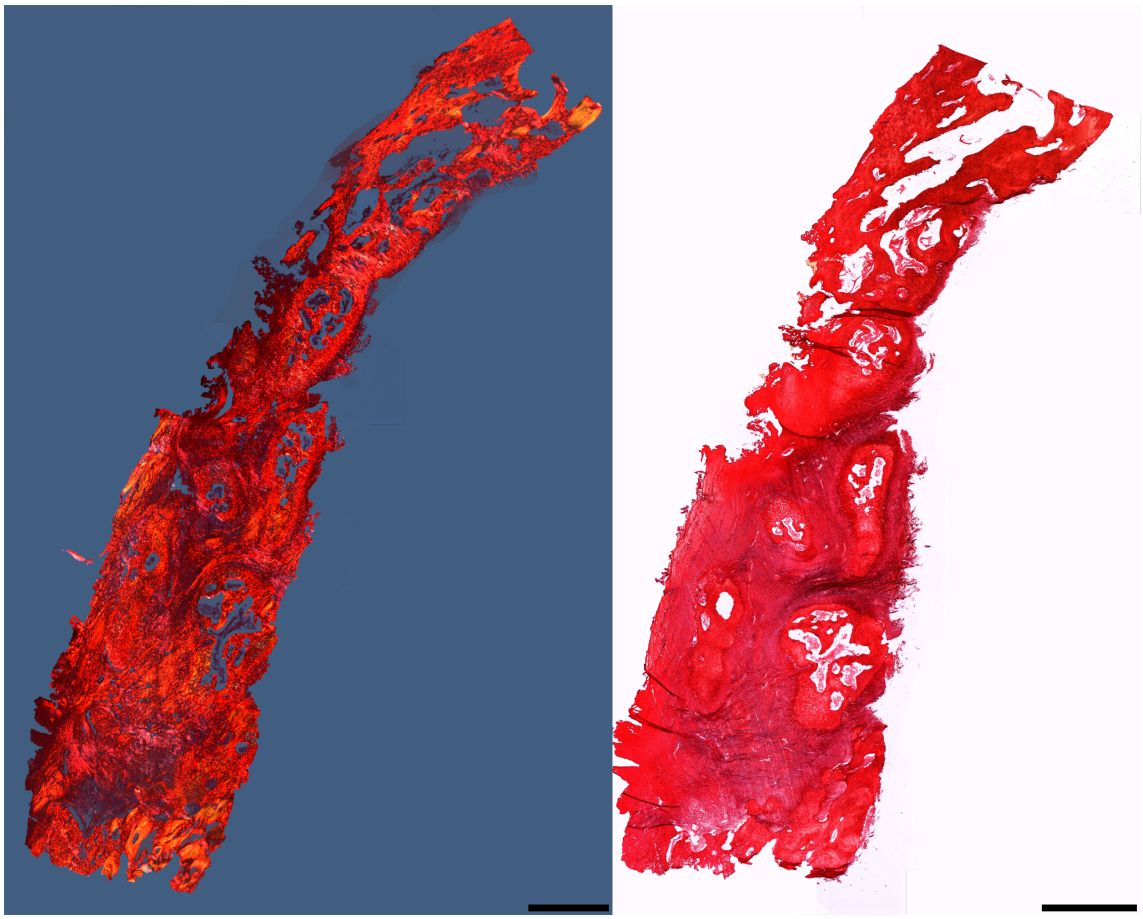

Figure 9: PSR-stained images of specimen 2 depicting an ossified suture region. Left image is a view under polarized light and right image depicts the ossified region with normal light microscopy. Polarization shows presence of collagen. Scale bar in all images = 1 mm.

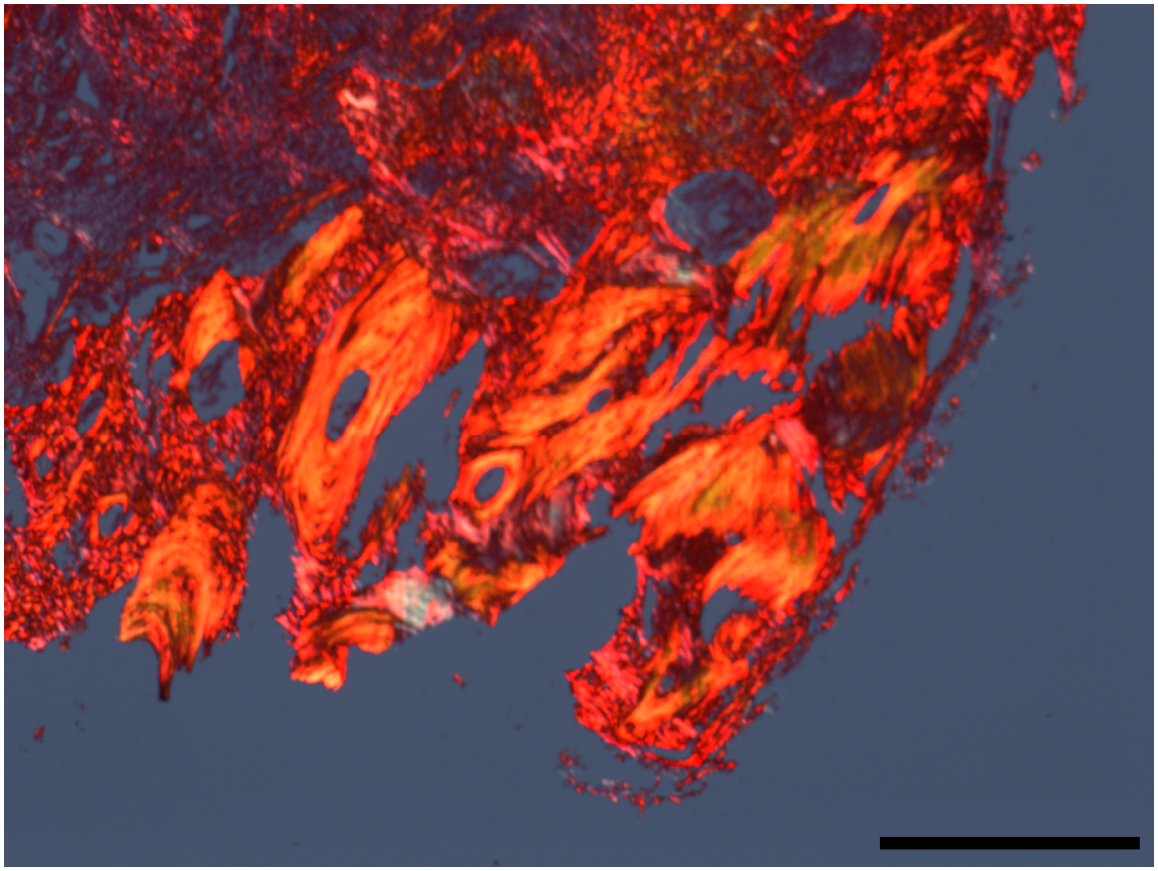

Figure 10: Ossified region of specimen 2 viewed using polarized light microscopy. Presence of collagen is indicated by birefringence (bright yellowish-red and green appearance) in this closed suture tissue. There is a repeating pattern of bright and dark bands in some areas of the section (arrows). Scale bar = 500 μm.

Picriosirius red, a stain utilized in this study, was applied for histological visualization of type I and III collagen fibers. Under polarized light, collagen fibers found in the tissue appeared bright red-orange and green and could be distinguished from the non-collagenous background material, which appeared black. Because bone is composed of roughly 30% organic compounds, of which collagen constitutes about 90%, the presence of collagen provides the principal supporting framework of the suture.

Specimen 3, obtained from a two-month-old child, was divided into five areas of interest, sagittal anterior and posterior (partially ossified), sagittal center (ossified), and a coronal and lambdoid region, and was stained using picrosirius red and alcian blue to assess tissue morphology. This stain was useful for visualizing the suture site and its surrounding areas where bone was thought to be deposited.

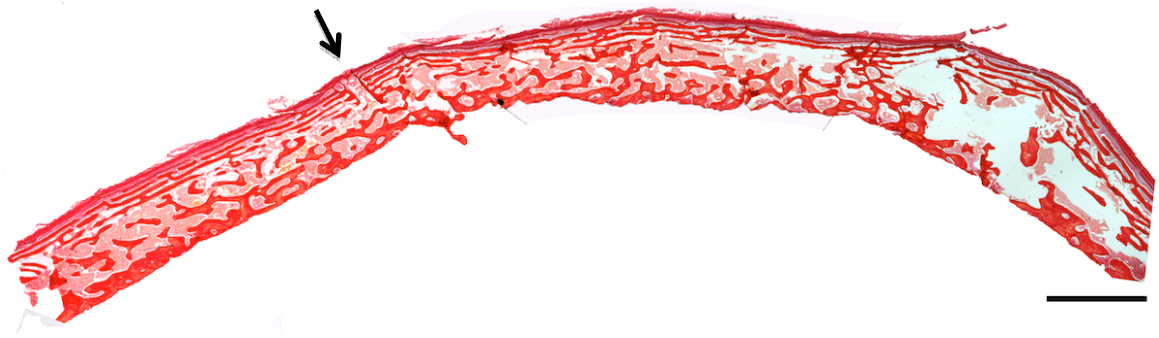

Figure 11: Sagittal posterior, partially ossified region of specimen 3 stained using picrosirius red and alcian blue stain and viewed using light microscopy. The area depicts a possible fusing suture shown by the prominent gap found in the tissue and indicated by the arrow. There is also the presence of several thin, parallel layers of cortical bone adjacent to trabecular bone. Scale bar = 1 mm.

Interestingly, the sagittal posterior (partially ossified) region of specimen 3 displayed an organized layering pattern on its periosteum side, while trabecular bone appeared deeper into the suture (toward the dura mater). The tissue also exhibited a region where it seemed that parietal bone plates were meeting and undergoing fusion. This feature can be seen by a distinctive gap in the tissue (Figure 12).

At the microscopic level, flat bones of the skull have outer compact bone layers, one layer toward the periosteum and the other toward the brain. Cancellous (trabecular) bone occupies the center region between the two layers. The results obtained from picrosirus red and alcian blue staining demonstrated these two types of bone, trabecular and compact, present in the cranial suture tissue (Figure 12). The compact bone could be forming at the site of suture fusion, a possibility that is supported by results shown in Figure 13.

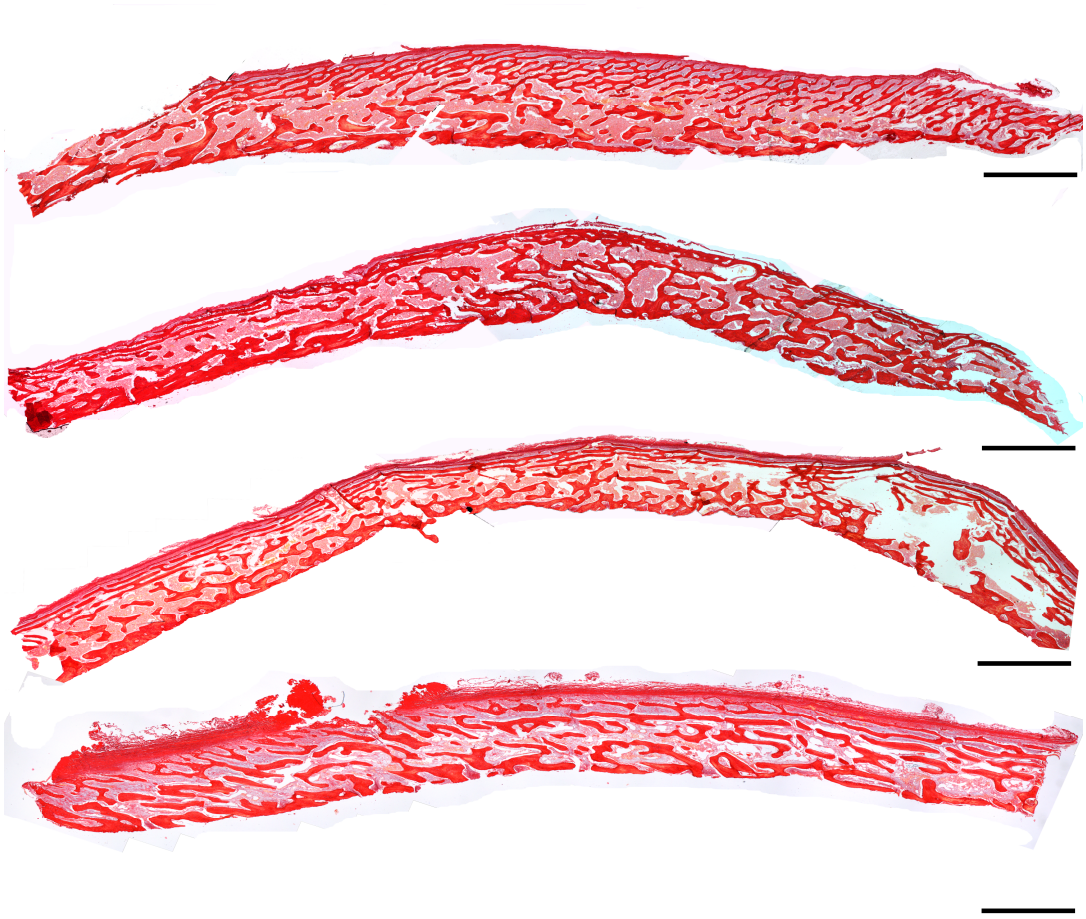

Figure 12: This figure depicts photomicrographs obtained from a surgical sample of a male, three-month-old child (specimen 3) and stained with picrosirius red and alcian blue. The first, second, third, and last micrographs depict a coronal, a sagittal center (ossified), a posterior (partially ossified) and a lambdoid suture region, respectively. Note that an anterior sagittal suture is not depicted. Scale bar = 1 mm.

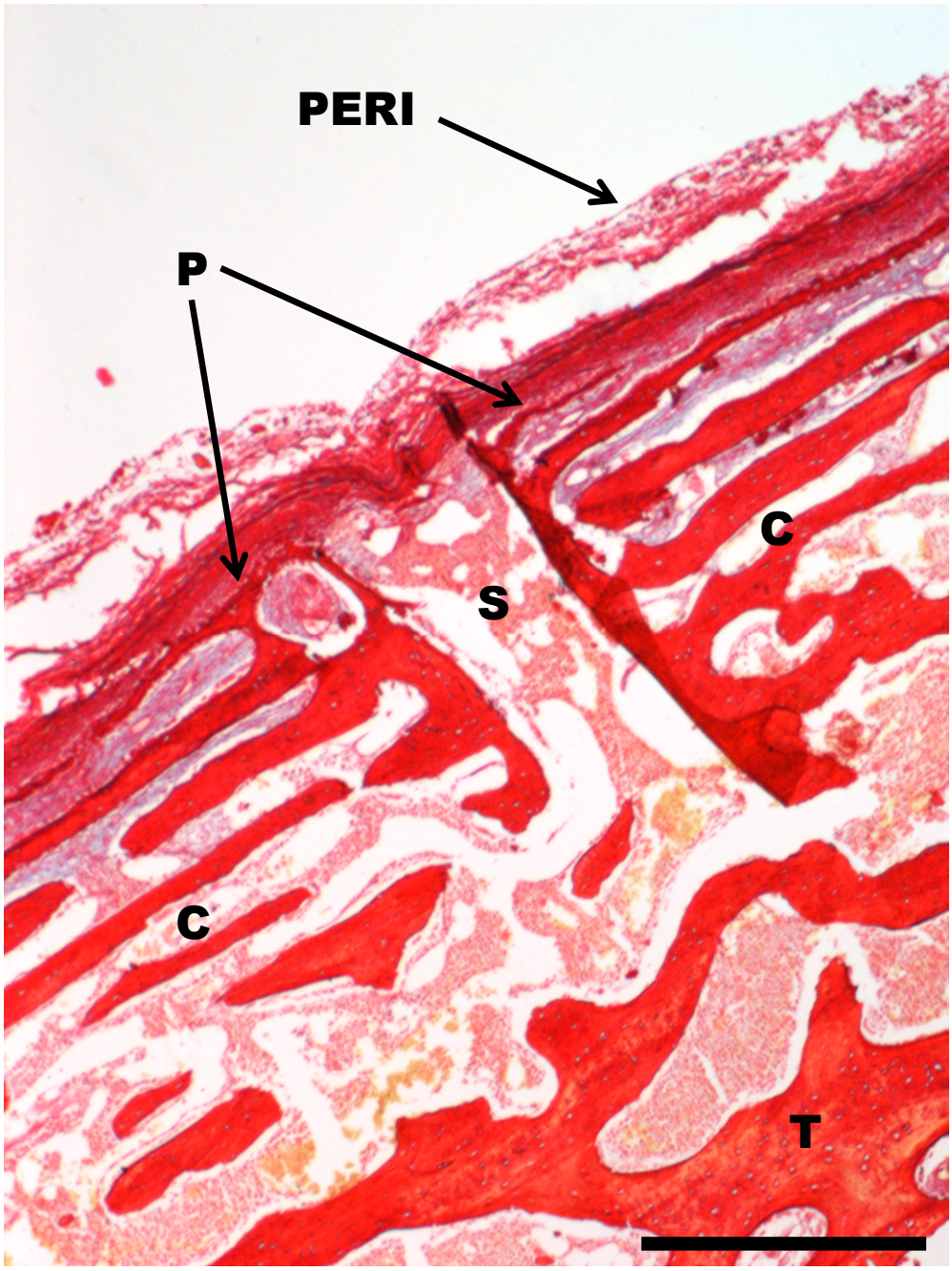

Figure 13: Enlargement of Figure 11, the sagittal posterior, partially ossified suture region displaying a layering pattern of cortical bone (C) near the periosteum surface with a possible open, unfused area (S) in the center of two opposing parietal bone plates (P). Trabecular bone (T) is deposited deeper into the tissue. Scale bar = 500 µm.

The gap that appeared within the layered cortical bone evidently depicted an area of the suture tissue that was open and undergoing ossification (Figure 11). It is presumed that the suture joint would eventually ossify when parietal plates met from opposing sides. Once the bone ossified, the suture would disappear and would leave no trace of the suture site. This open region normally provides continued growth of the skull but such regions are diminished or lost in premature suture fusion, as previously noted. Once a suture site disappears, it becomes impossible to identify its location in the ossified tissue. This result explains why suture sites cannot be identified in other closed areas of the surgical specimens examined in this study.

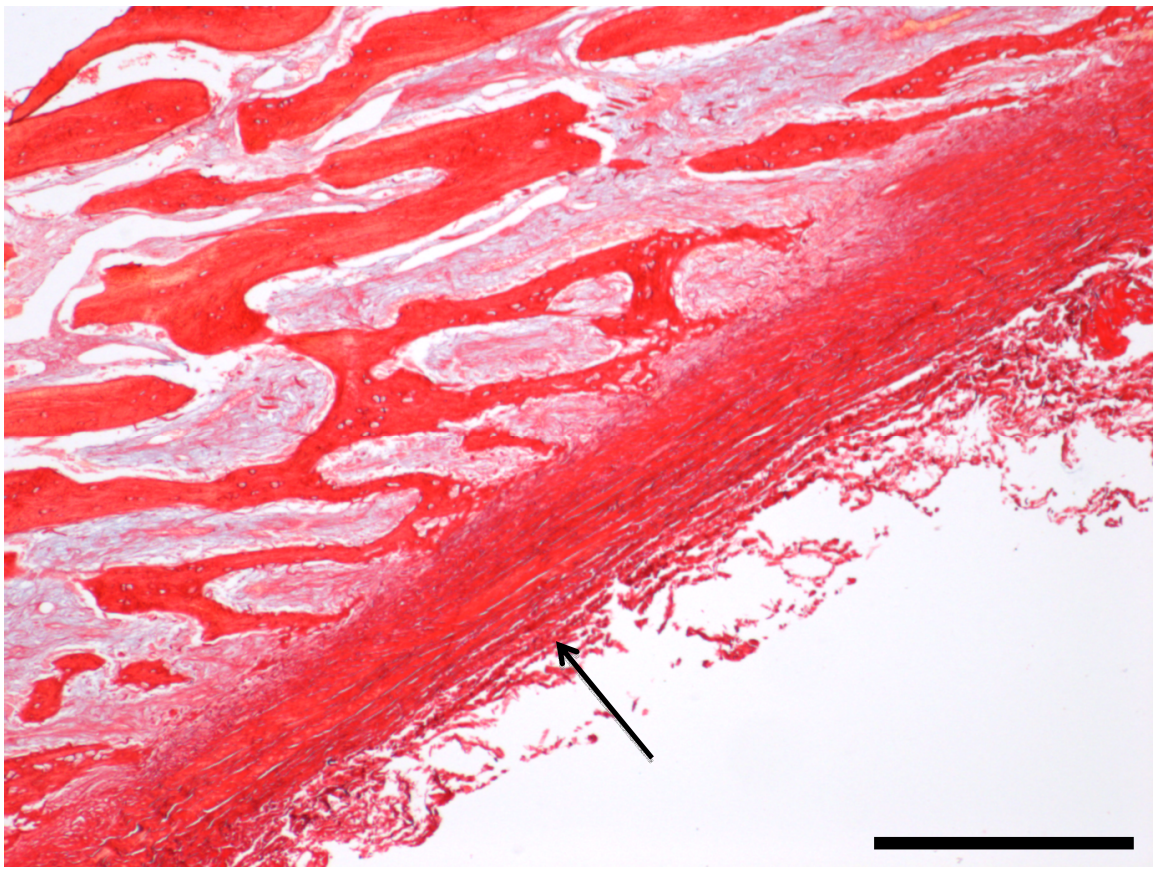

Figure 14: Image taken from a lambdoid suture region showing periosteum surrounding the outside of the skull bone (toward the skin), as indicated by the arrow. The periosteum is a layer of dense connective tissue and is fibrous externally (toward the skin) but becomes more vascularized and cellularized near the bone tissue. Scale bar = 500 μm.

Trabecular bone is known to be very sensitive to external forces and provides the remarkable strength of the skull. This type of bone is extremely porous and forms the inner area of the skull bones, whereas compact (cortical) bone forms the outer layers. This description agrees with the histological results obtained in this study using picrosirius and alcian blue staining. All areas of interest, sagittal anterior and posterior (partially ossified), sagittal center (ossified), and a coronal and lambdoid region, displayed this type of tissue arrangement, where the periosteum side of the samples contained cortical bone and inner bone layers were trabecular (Figure 12).

Osterix, a zinc-finger containing transcription factor essential for forming bone, was identified and localized in cranial suture tissue in specimen 4. Osterix is specifically found in the nucleus of cells undergoing the transition between mesenchymal stem cells and osteoblasts, as it is a protein that plays a role in the transcription of other important proteins vital to bone development and the differentiation of mesenchyme cells into osteoblasts. Figures 15 -18 are images of osterix immunohistochemical staining of a posterior, sagittal suture region from a four-month-old male. The staining demonstrates the presence of osterix in cells transition to osteoblasts of this developing suture tissue. Counterpart sagittal suture sections treated without primary antibody to osterix were negative controls and they showed no specific staining for osterix (Figures 15 -16). Such negative controls verify that the immunostaining of osterix is real and not the result of a nonspecific reaction.

In detail, immunostaining results indicated the presence of osterix in cells lining the surfaces of trabecular bone and the absence of osterix in cells of cortical bone (Figure 15). 3,3'-diaminobenzidine (DAB) staining was present also within posterior portions of the trabecular bone of sagittal sutures, a result indicative of osterix and thus osteoblast activity in this suture region (Figure 15).

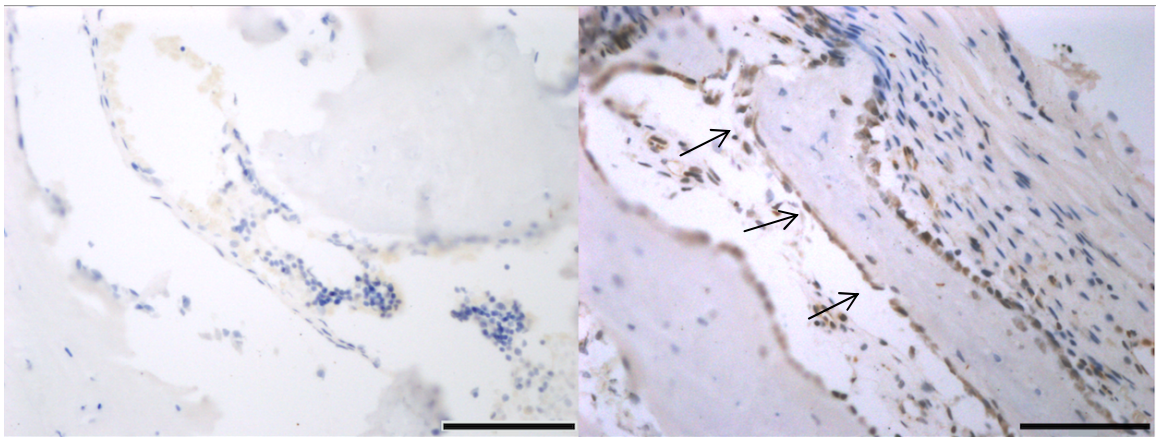

Figure 15: Immunohistochemistry of osterix-stained images from a four-month-old male (specimen 4), showing posterior portions of a sagittal suture. The image on the left shows a negative control test area where DAB staining for osterix is absent because no primary antibody was applied to the tissue. The image on the right shows a region of the posterior, sagittal suture reacted with primary antibody. DAB staining (brown) is present in this suture region within osteoblasts lining the trabecular bone (arrows) and within cells found in marrow spaces (arrowheads). Scale bar = 500 μm.

On comparison of negative control test slides and experimental slides, mesenchymal stem cells (MSC) were found to be present in the marrow space in both (Figure 16). In the negative controls, the MSCs stained blue with hematoxylin, whereas in the experimental slides MSCs stained brown (DAB staining) as well as blue, an observation that verified the presence of osterix. This finding was notable in that it supported the notion that intramembranous

ossification was occurring. MSCs are progenitor cells that may become osteoblasts under certain conditions, and osterix staining demonstrated the transition from MSCs to osteoblasts in the marrow spaces. These osteoblasts or their precursors appear to form a nidus, a dense cluster of cells within the marrow spaces. Differentiated osteoblasts, stained brown for osterix, are lining the trabecular surfaces of the suture (Figure 16).

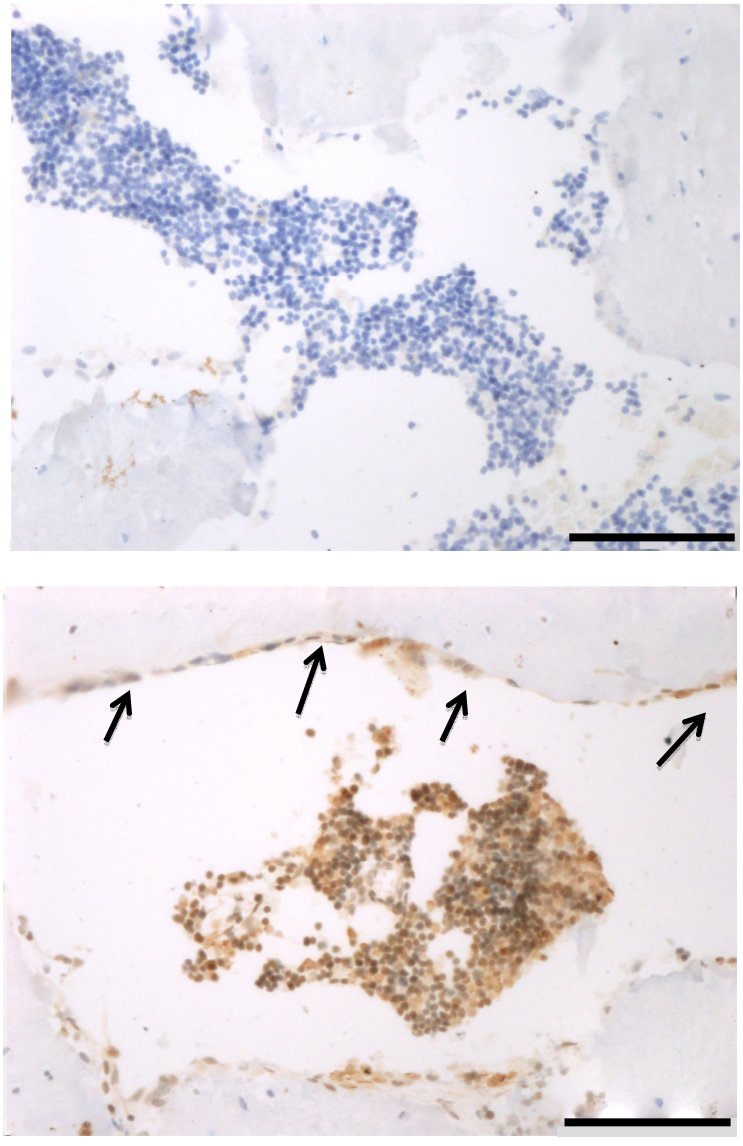

Figure 16: Posterior portions of a sagittal suture from a four-month-old male stained without (upper panel) and with (lower panel) DAB to demonstrate osterix. Images are taken from the same region of the specimen but different areas within the tissue. Aggregation of mesenchymal stem cells appears in the marrow space as can be seen by the cluster of cells in the center of the tissue. The nidus of aggregated cells in the marrow space in the lower panel is composed in part by DAB-stained cells transitioning from MSCs to osteoblasts. Differentiated osteoblasts line the trabecular bone as indicated by the arrows. Scale bar = 500 μm.

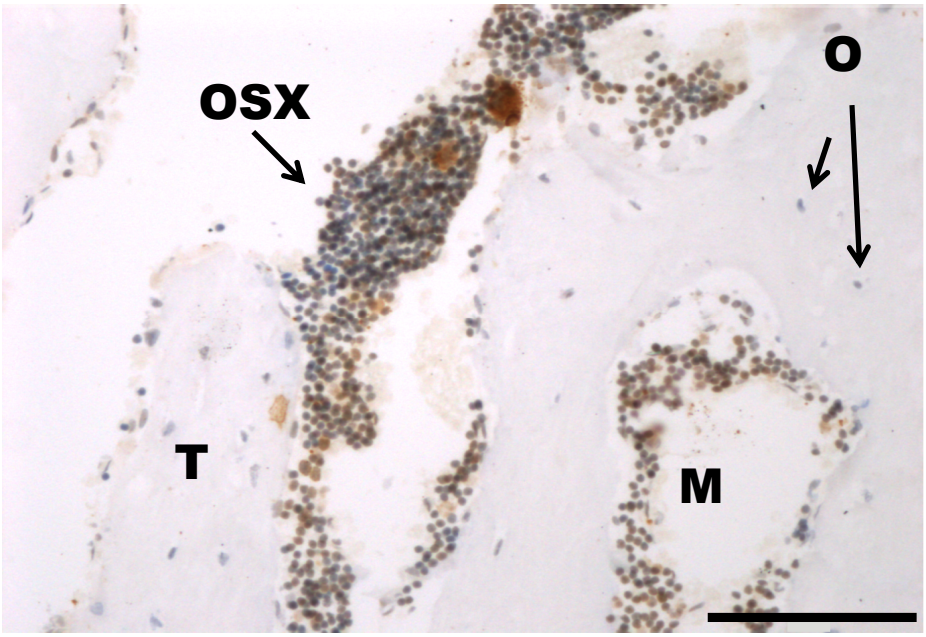

Figure 17: Posterior portions of a sagittal suture from a four-month-old male stained with DAB to demonstrate osterix. The image shows osterix staining in the marrow spaces of the tissue. T = trabecular bone. M = marrow space. OSX = osterix stain. O = osteocytes. Scale bar = 500 μm.

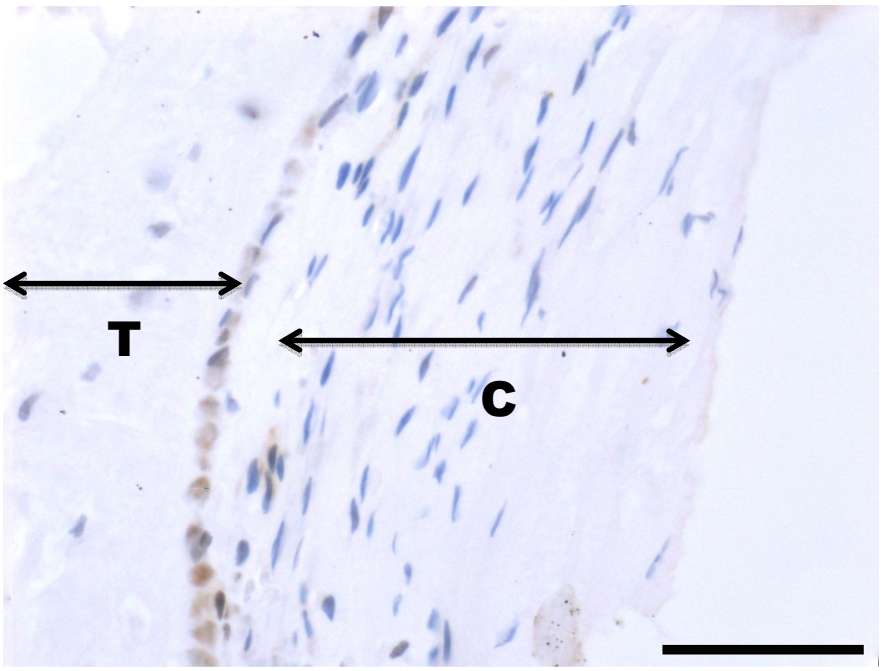

Figure 18: Posterior portions of a sagittal suture from a four-month-old male stained with DAB to demonstrate osterix. The DAB stain remains particular to the osteoblasts lining the trabecular bone region and is absent in cells within cortical bone. C = cortical bone. T= trabecular bone. Scale bar = 500 µm.

Overall, the novel finding of osterix in the suture tissue from specimens of craniosynostosis supports the concept that osteoblast activity and bone formation occur in or around the closing suture. As a transcription factor, osterix acts as a marker for osteoblast differentiation and proliferation in postnatal bone formation of the skull. Additionally, the absence of osterix expression in cortical bone and the presence of osterix in cells lining the surfaces of trabecular bone as well in cell aggregates within trabecular bone marrow spaces are new findings.

Discussion

Craniosynostosis, the premature fusion of the suture(s) in pediatric patients, is a pathological condition that remains ambiguous and incompletely understood.

Although studies with syndromic (with known condition) craniosynostosis have identified genetic factors associated with this condition, little is known about the nonsyndromic form of craniosynostosis. This research study intended to understand more thoroughly cranial suture biology and the deformational factors leading to the diseased phenotypes in nonsyndromic forms of craniosynostosis. Results of gross morphology and histology of affected suture tissues were obtained to provide structural and architectural information about the specimens. In addition, immunohistochemistry of osterix yielded the preliminary result that this transcription factor was associated with cells in aggregates within marrow spaces of the tissues as well cells lining the trabecular areas of the sutures. The presence of DAB-positive cells in marrow spaces provides evidence that MSCs transition to osteoblasts in these trabecular bone regions. Cells lining the trabecular suture areas are also DAB-positive and here they are functional, differentiated osteoblasts. Further, osterix expression is absent in cortical bone. The findings of osterix in osteoblasts at the trabecular surfaces of the sutures and in cell aggregates within marrow spaces of trabeculae have not been reported previously. These results provide new insight into craniosynostosis and cranial suture biology.

Future studies will examine osterix immunohistochemistry more completely to understand the formation of trabecular bone in additional sagittal sutures affected by craniosynostosis as well as synostoses in other bones of the skull. Efforts will also be made to quantitate expression of osterix in diseased tissue, so comparisons could be made to control tissue regions (normal suture areas

extracted alongside fused regions during surgery). If expression levels of the osterix protein were abnormally higher in fused suture regions compared to that of open regions, then it might be concluded that high osterix expression plays a role in suture closure. If such were the case, proteins upstream of osterix would also be analyzed and would include Indian Hedgehog (IHH), Wnt, and Runx2. These proteins might themselves have downstream effects on osterix. A high level of osterix expression could possibly influence the rate of differentiation and the number of osteoblasts in the suture tissue region leading to bone deposition.

As discussed before, the lack or inactivation of osterix can have detrimental effects causing severely undeveloped bone anatomy of the skull in mice (Baek *et al.,* 2009). In the present study, results propose that overexpression or upregulation of osterix could potentially also lead to detrimental effects resulting in overdevelopment and premature fusion of the bone tissue. Craniosynostosis could be one such effect. Future work will hopefully provide greater insight into the etiology of craniosynostosis. Again, surgical specimens would be collected from Akron Children's Hospital, dissected, processed, embedded, and sectioned for analysis.

It is already known that osterix knock-out mice fail to form bone but to understand further the role of osterix in normal bone development, a mouse model could be studied. One model is the mice affected with Frank-ter Haar syndrome, which is known to induce sagittal craniosynostosis (Bendon *et al.,* 2012). This mouse model would allow thorough examination of both a fully diseased and normal tissue sample from calvaria. Such a mouse model would

overcome the limitation of the present study in which normal sagittal human tissue from a perfectly healthy skull of an infant cannot be obtained in any surgical instance. Frank-ter Haar mice, however, could still be used for comparison with tissue from normal mouse counterparts. It is difficult to mimic the nonsyndromic form of craniosynostosis in mice because the cause of the nonsyndromic form, as its name implies, is unknown and therefore impossible to induce in the animals.

RNA levels of osterix could be measured in diseased and normal tissue through RNA isolation and polymerase chain reaction (PCR) analysis. If osterix RNA expression were statistically different between the diseased and normal tissue, then molecular genetics could be used to investigate genes encoding the osterix protein in the diseased and normal states.

The discovery of osterix in the human craniosynostosis diseased tissue here introduces new avenues and possibilities for understanding the condition more completely. It would be interesting to study the molecular and cellular mechanisms that govern osterix control of how and when osteoblast proliferation and differentiation occur, as these are areas that remain uncertain. It is known that osterix is present in the early stages of osteoblast proliferation and differentiation, whereas proteins like osteocalcin, osteopontin and bone sialoprotein are mid-to-late stage osteoblast markers. Thus osterix effects on the complete osteoblast pathway (early to final stages) need to be investigated. Additional studies addressing the role of osterix in the pathway could provide clearer insight about craniosynostosis and possibly other bone pathologies.

The current treatment of craniosynostosis remains traditional surgery (ranging from minimal to invasive). The goal of corrective surgery is to treat the pathology once it has already formed. This surgery allows any pressure on the brain to be relieved/removed, provides ample room for the growth of the skull, and can improve the appearance of the child. This condition can be inherited but most cases remain sporadic. Therefore genetic counseling could be recommended to those families that are aware of the inherited disorder. Continued research efforts should be made to understand craniosynostosis, so the disease can be prevented before it even occurs. Progress should be made to prevent this problem rather than treating it after the fact. Like folic acid taken as a prenatal vitamin during pregnancy to help prevent birth defects of the brain and spinal cord, perhaps in the future a similar type of treatment or drug will be recommended to pregnant women to prevent diseases like craniosynostosis in infants.

In conclusion, this study used histological and/or immunohistochemical analyses to study nonsyndromic sagittal synostoses as well as patent (normal open suture) tissue obtained from the skulls of three pediatric patients in surgery from Akron Children's Hospital. Histological staining, including toluidine blue, hematoxylin and eosin, and picrosirius red counterstained with alcian blue, has been performed. The histological methods provided qualitatively describing tissue and cell architectural shapes and gross morphology of surgical specimens. Immunohistochemical analyses were also performed to study the presence of osterix, and the preliminary results found osterix presence in posterior portions of

the sagittal regions of the specimens of interest. This finding is novel. Osterix, a critical transcription factor in bone, is known to play a vital role in osteoblast differentiation and bone formation. Continued progress in understanding osterix gene expression and protein synthesis and secretion will be particularly important for gaining information and insight into craniosynostosis.

Acknowledgments

The authors are thankful for the assistance in technical help given by Mr. Joshua Bundy (Department of Polymer Science, University of Akron) and by Dr. Hitomi Nakao (Department of Plastic and Reconstructive Surgery, Kinki University School of Medicine, Osaka, Japan). The authors also thank the Akron Children's Hospital for the collection of surgical samples and the donors and their parents for providing the tissues for investigation.

References

Baek, W-Y, M Lee, JW Jung, S-Y Kim, H Akiyama, BD Crombrugghe, and JE Kim. "Positive Regulation of Adult Bone Formation by Osteoblast-Specific Transcription Factor Osterix." *Journal of Bone and Mineral Research* 2009; 24: 1055-065.

Bendon, C, A Fenwick, J Hurst, G Nürnberg, P Nürnberg, S Wall, A Wilkie, and D Johnson. "Frank-ter Haar Syndrome Associated with Sagittal Craniosynostosis and Raised Intracranial Pressure." *BMC Med Genet BMC Medical Genetics* 2012; 13: 104.

Bronfin, DR. "Misshapen Heads in Babies: Position or Pathology?" *Ochsner Journal* 2001; 3: 191-99.

Connerney, J, V Andreeva, Y Leshem, M Mercado, K Dowell, X Yang, V Lindner, R Friesel, and D Spicer. "Corrigendum to “Twist1 Homodimers Enhance FGF Responsiveness of the Cranial Sutures and Promote Suture Closure.” *Developmental Biology* 2008; 318: 323-334.

Day, TF, and Y Yang. "Wnt and Hedgehog Signaling Pathways in Bone Development." *Journal of Bone and Joint Surgery* 2008; 90: 19-24.

Kolpakova-Hart, E, B McBratney-Owen, B Hou, N Fukai, C Nicolae, J Zhou, and BR Olsen. "Growth of Cranial Synchondroses and Sutures Requires Polycystin-1." *Developmental Biology* 2009; 321: 407-19.

Levi, B, DC Wan, VW. Wong, E Nelson, J Hyun, and MT. Longaker. "Cranial Suture Biology: From Pathways to Patient Care." *Journal of Craniofacial Surgery* 2012; 23: 13-19.

Morriss-Kay, G M., and A O. M. Wilkie. "Growth of the Normal Skull Vault and Its Alteration in Craniosynostosis: Insights from Human Genetics and Experimental Studies." *Journal of Anatomy* 2005; 207: 637-53.

Tan, SH, K Senarath-Yapa, MT. Chung, MT. Longaker, JY. Wu, and R Nusse. "Wnts Produced by Osterix-expressing Osteolineage Cells Regulate Their Proliferation and Differentiation." *Proceedings of the National Academy of Sciences* 2014; 49: 17354.

Sbazo-Rogers, H, MB. Rogers, SK. Schulze, BJ. Cusack, JM. Tabler, WB. Barrell, and KJ. Liu. “Regional Identity controls osteogenesis in the embryonic skull.” *Center for Craniofacial Regeneration* 2014 (Abstract).

Zhu, F, MS. Friedman, W Luo, P Woolf, and KD. Hankenson. "The Transcription Factor Osterix (SP7) Regulates BMP6-Induced Human Osteoblast Differentiation." *Journal of Cellular Physiology* 2012; 227: 2677-685.